PHILOSOPHICAL TRANSACTIONS B

royalsocietypublishing.org/journal/rstb

Research

Cite this article: Graham OJ *et al*. 2023 Deeper habitats and cooler temperatures moderate a climate-driven seagrass disease. *Phil. Trans. R. Soc. B* **378**: 20220016.
https://doi.org/10.1098/rstb.2022.0016

Received: 19 August 2022
Accepted: 25 November 2022

One contribution of 15 to a theme issue 'Infectious disease ecology and evolution in a changing world'.

Subject Areas:
ecology, health and disease and epidemiology

Keywords:
eelgrass, marine disease, seagrass wasting disease, *Labyrinthula zosterae*, climate change, climate refugia

Author for correspondence:
Olivia J. Graham
e-mail: ojg5@cornell.edu

Deeper habitats and cooler temperatures moderate a climate-driven seagrass disease

Olivia J. Graham[1], Tiffany Stephens[2], Brendan Rappazzo[3], Corinne Klohmann[1], Sukanya Dayal[4,5], Emily M. Adamczyk[6], Angeleen Olson[7], Margot Hessing-Lewis[7], Morgan Eisenlord[1], Bo Yang[8], Colleen Burge[9,10,†], Carla P. Gomes[3] and Drew Harvell[1]

[1]Department of Ecology and Evolutionary Biology, Cornell University, Ithaca, NY 14853-0001, USA
[2]Seagrove Kelp Co, Ketchikan, AK 99901, USA
[3]Department of Computer Science, Cornell University, Ithaca, NY 14850, USA
[4]Department of Natural Resources, Cornell University, Ithaca, NY 14853, USA
[5]Department of Biology and Marine Biology, University of North Carolina, Wilmington, NC 28403-5915, USA
[6]Department of Zoology and Biodiversity Research Centre, University of British Columbia, Unceded xʷməθkʷəy̓əm (Musqueam) Territory, Vancouver, British Columbia, Canada V6T 1Z4
[7]Hakai Institute, Calvert Island, P.O. Box 25039, Campbell River, British Columbia, Canada V9W 0B7
[8]Department of Urban and Regional Planning, San Jose State University, San Jose, CA 95112, USA
[9]Institute of Marine and Environmental Technology, University of Maryland Baltimore County, Baltimore, MD 21202, USA
[10]Department of Microbiology and Immunology, University of Maryland Baltimore, Baltimore, MD 21201, USA

OJG, 0000-0003-3834-264X; TS, 0000-0001-6422-1003; CK, 0000-0003-4572-1226; EMA, 0000-0002-3778-9434; AO, 0000-0001-8443-1868; MH-L, 0000-0002-9956-955X; ME, 0000-0002-9353-6642; BY, 0000-0001-7439-192X; CB, 0000-0002-9793-9801; CPG, 0000-0002-4441-7225; DH, 0000-0002-8905-9847

Eelgrass creates critical coastal habitats worldwide and fulfills essential ecosystem functions as a foundation seagrass. Climate warming and disease threaten eelgrass, causing mass mortalities and cascading ecological impacts. Subtidal meadows are deeper than intertidal and may also provide refuge from the temperature-sensitive seagrass wasting disease. From cross-boundary surveys of 5761 eelgrass leaves from Alaska to Washington and assisted with a machine-language algorithm, we measured outbreak conditions. Across summers 2017 and 2018, disease prevalence was 16% lower for subtidal than intertidal leaves; in both tidal zones, disease risk was lower for plants in cooler conditions. Even in subtidal meadows, which are more environmentally stable and sheltered from temperature and other stressors common for intertidal eelgrass, we observed high disease levels, with half of the sites exceeding 50% prevalence. Models predicted reduced disease prevalence and severity under cooler conditions, confirming a strong interaction between disease and temperature. At both tidal zones, prevalence was lower in more dense eelgrass meadows, suggesting disease is suppressed in healthy, higher density meadows. These results underscore the value of subtidal eelgrass and meadows in cooler locations as refugia, indicate that cooling can suppress disease, and have implications for eelgrass conservation and management under future climate change scenarios.

This article is part of the theme issue 'Infectious disease ecology and evolution in a changing world'.

1. Introduction

The increasing incidence and severity of disease outbreaks [1–3]—fuelled by acute and prolonged warming ocean temperatures [1,4–9]—makes marine disease ecology a priority in the portfolio of climate change research. Temperature-sensitive pathogens that target marine foundation species like corals and eelgrass (*Zostera marina*), a temperate seagrass species, can be especially devastating, given their pivotal

†Present address: California Department of Fish & Wildlife, University of California Davis Bodega Marine Laboratory, Bodega Bay, CA 94923, USA.

Electronic supplementary material is available online at https://doi.org/10.6084/m9.figshare.c.6360115.

THE ROYAL SOCIETY PUBLISHING

roles in driving marine ecosystem structure and function [7,9–11]. Eelgrass has the largest global distribution of any marine angiosperm, and grows in shallow, coastal areas throughout the Northern Hemisphere, spanning from Baja, Mexico to Alaska [12]. Seagrass wasting disease, caused by the protist *Labyrinthula zosterae*, is one of the current threats to the health and sustainability of global seagrass meadows [13,14]. The pathogen consumes plant chloroplasts [15], impairs photosynthesis [16], produces distinctive black lesions [17–19] and reduces eelgrass growth and belowground sugar stores in natural meadows [20]. Historical disease outbreaks in the 1930s reduced some eelgrass meadows along the Atlantic coasts by 90% and dramatically altered their structure and function [21,22], reducing waterfowl and invertebrate populations [21,23–25], and altering the water quality in coastal regions [26]. Eelgrass disease outbreaks continue to persist in temperate seas worldwide [9,27–32], and can result not only in local extinctions, but also in the loss of the valuable ecosystem services eelgrass provides: carbon sequestration, sediment stabilization, water filtration, nutrient cycling and habitat formation [33–35].

Warming ocean temperatures and wasting disease can independently and synergistically interact and harm eelgrass. Rising temperature, including increased frequency and intensity of marine heatwaves [36], is among the most prominent global change factors impacting seagrass ecosystems [37,38], which are declining globally [39]. Warmer temperatures are associated with dramatic reductions in eelgrass growth [40,41], net primary production [42], density [8,43] and biomass [44]. Dramatic examples include widespread mortality of eelgrass in the Chesapeake Bay, Virginia, USA [42] and other seagrass in Western Australia [45] from marine heatwaves. Following recent marine heatwaves, shallower, warmer estuaries also had reduced eelgrass biomass compared to deeper, cooler estuaries [46]. Further, warmer temperatures under climate change projections are expected to substantially shift eelgrass ranges northwards and increase eelgrass susceptibility to anthropogenic and natural stressors like disease [47].

Along with rising temperatures, seagrass wasting disease is among one of many multiple stressors threatening global seagrass meadows [14,48]. Climate change is predicted to increase disease impacts on eelgrass health and meadow resistance [14]. Certain abiotic conditions—including warm temperatures—were implicated in historic wasting disease outbreaks [26,49,50]. More recently, elevated temperatures were associated with higher disease levels in natural meadows [9,27,32]. Field surveys also suggest interactions between wasting disease and ocean temperatures facilitated seagrass declines in Sicily, Italy [27] and Washington State, USA [9,51]. Laboratory experiments demonstrate the causative agent, *L. zosterae*, grows faster at warmer temperatures up to 25°C [52,53], though the exact mechanisms underlying this relationship remain unknown [54]. Certain eelgrass biometrics are also associated with greater wasting disease. Field surveys detected significant, positive correlations between disease metrics and eelgrass leaf area and negative correlations between disease and shoot density [9,29,30]. Many other environmental parameters influence eelgrass health and survival (e.g. exposure to waves and desiccation stress, salinity, sediment), though temperature, light and nutrients are the most important for eelgrass health and productivity [40,55,56]. Despite the growing understanding of the role of climate and other environmental drivers on wasting disease, little is known about factors that lead to better outcomes for natural meadows, such as cooler, higher latitudes or deeper water.

To capture a broad range of environmental conditions, better understand the synergistic effects of climate and disease on this foundation species, and determine the potential for cold, deep refugia, disease surveys spanning a wide latitude and depths in the northern range of eelgrass distribution are essential. Previous studies reported that disease was lower in deeper eelgrass meadows in the San Juan Islands, Washington (−4 m mean lower low water) and Sweden (−2 to −5 m) [29,31]. This suggests the hypothesis that deeper, subtidal eelgrass meadows may provide plants with more favourable climatic conditions—and less favourable conditions for the pathogen—that allow them to persist [57,58]. Similar patterns were found among three species of algae, which had more severe infections in shallower regions compared to those at depth [59]. Refugia from climate change and disease pressure could potentially mitigate local extinctions owing to disturbances [58]. Already, deeper habitats serve as refugia from marine heatwaves for seaweeds [60], corals [61], temperate reefs [62] and eelgrass [46]. These examples highlight how deeper marine environments could reduce the impacts of climate change and pathogenic stressors, and exemplify the need to further understand host–pathogen interactions in these environments.

We aimed to test the following hypotheses: (i) disease prevalence and severity are reduced in meadows at higher latitudes with cooler temperatures. Prevalence is the proportion of surveyed leaves that are infected and severity is the proportion of leaf area that is visibly infected; (ii) disease levels are lower in deeper, subtidal eelgrass compared to the more environmentally stressful conditions of shallower, intertidal eelgrass; and (iii) disease is higher in high-density eelgrass meadows, since the disease transmits via direct contact with infected leaves [15]. To address these, we surveyed seagrass wasting disease in eelgrass meadows throughout their northern range from Puget Sound, Washington to southeast Alaska in the northeast Pacific to explore how disease varied across eight degrees latitude, tidal zones (intertidal or subtidal), environments, and time. Altogether, we surveyed 5761 eelgrass leaves from paired, adjacent intertidal and subtidal eelgrass meadows for leaf-specific measurements (leaf area, disease prevalence and severity) and site-specific biometrics (density and canopy height). Intertidal eelgrass meadows are exposed to more stressful, extremely variable environmental conditions at low tide, including higher temperatures, desiccation, ultraviolet (UV) stress, and at high latitudes, scouring by sea ice [63,64]. By contrast, deeper, subtidal meadows are constantly submerged and have more stable environmental conditions. Just as environmental conditions can vary dramatically with elevational gradients and influence disease dynamics on land [65]—so too can the environment and disease vary with depth in our oceans. Because intertidal eelgrass is exposed at low tide to greater environmental stressors, it could be more vulnerable to infection in a changing climate. Intertidal environments could also be more conducive to pathogen growth. Given that relatively little is known about disease at depth [31], we made investigation of subtidal disease a key research priority in this project.

2. Methods

(a) Field surveys

We surveyed 19 intertidal and subtidal eelgrass meadows across four geographical regions: southeast Alaska; British Columbia,

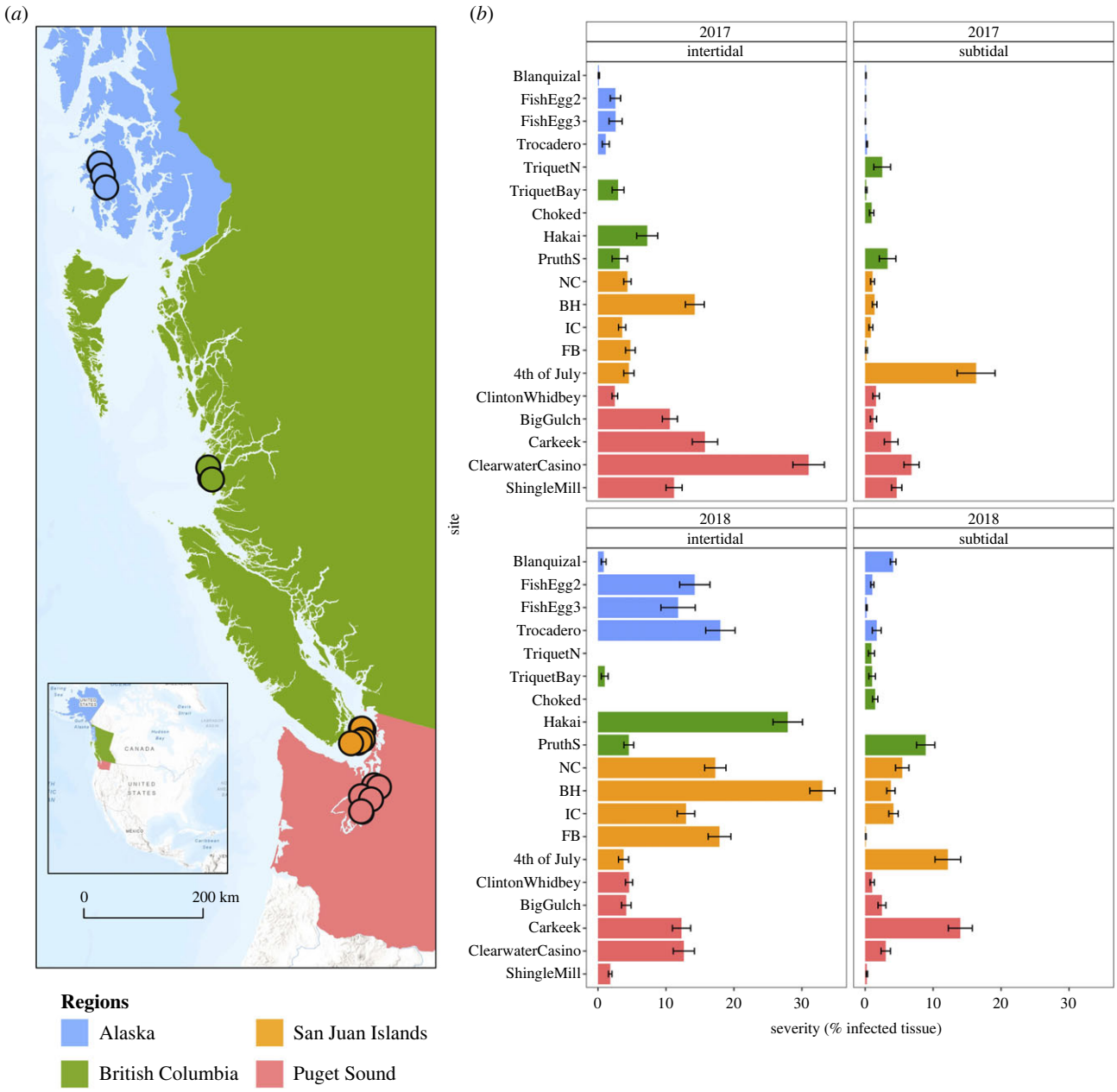

Figure 1. (*a*) Locations for seagrass wasting disease surveys in Alaska, British Columbia, San Juan Islands and Puget Sound in summers 2017 and 2018. Surveys included paired subtidal and intertidal eelgrass meadows. Map made in ArcGIS. (*b*) Site-level disease severity reflect lower disease in subtidal meadows and generally higher disease in 2018; $n = 5761$ blades (mean ± s.e.). Sites are arranged north to south, top to bottom within and by regions. Sites with missing bars did not have eelgrass and do not represent that there was not any disease present (intertidal: Triquet N, Choked; subtidal: Hakai).

Canada; San Juan Islands, Washington; and Puget Sound, Washington (figure 1*a*; electronic supplementary material, figure S1, table S1). Regions spanned sea surface temperature gradients and ranged from urban environments with high human impacts to remote environments with minimal to no development. For example, British Columbia sites were in the Hakai Lúxvbálís Conservancy, the largest marine protected area along coastal British Columbia (BC Parks), while Puget Sound sites in Washington were heavily urbanized, with some adjacent to a wastewater treatment plant and railroads. Surveys occurred in the summers of 2017 and 2018, when disease levels peak in temperate eelgrass [9,28,66,67]. Owing to logistical constraints, we had to stagger our sampling periods as such: we surveyed British Columbia in late June, Puget Sound in early July, San Juan Islands in mid-late July and Alaska in early August. Within a given region, we surveyed all sites on the same low-tide series.

In each region, we surveyed 3–5 paired intertidal and subtidal eelgrass meadows, except in British Columbia where three sites were strictly intertidal or subtidal. The San Juan Islands have a history of wasting disease monitoring [9,29,30] and recent, significant meadow declines [9,51,68]. For each field survey, we ran three, 20 m transects parallel to the shore in the middle of both intertidal and subtidal meadows. We sampled intertidal meadows at low tide and subtidal meadows using SCUBA or snorkeling (electronic supplementary material, Video 1). During 2017, we recorded the GPS coordinates at the ends of all intertidal transects for subsequent monitoring in 2018, so that we could compare the same parts of the meadows between years. We tracked subtidal transect locations using GPS coordinates from boats, dive compass headings, and in some cases, anchored subtidal transect markers. At each site, we haphazardly collected 120 intertidal and 60 subtidal leaves ($n = 40$ leaves per transect, $n = 20$ subtidal leaves per transect). Given the constraints of working underwater, the significantly larger size of subtidal eelgrass leaves compared to intertidal leaves, and the greater processing time required to process larger leaves, we collected fewer subtidal leaves. Intertidal meadows were at approximately +1 m and subtidal meadows were at depths ranging from approximately −1.8 to −6 m mean

lower low water. Because disease susceptibility and levels can vary with the age of eelgrass leaves [29], we standardized our collections to the third-rank (third youngest) leaf from each shoot, following other published approaches [9]. We measured densities and canopy height in three of the four surveyed regions: British Columbia, San Juan Islands, and Puget Sound; we took measurements from quadrats at three points along each transect (0, 10, 20 m). Owing to logistical constraints, we did not measure densities in any Alaska sites in either year nor subtidal Puget Sound meadows in 2018. We stored all leaves in bags with seawater on ice or in a refrigerator until processing for image analyses.

(b) Disease quantification

In the laboratory, we gently scraped epiphytes from eelgrass leaves using soft, flexible rulers. We scanned eelgrass leaves between two transparency sheets with a Canon CanoScan LiDE 220 scanner at 600 dpi resolution within 24 h of collection. This created digital images of eelgrass leaves for subsequent leaf area and disease measurements. Given that some subtidal leaves were nearly 3 m long, we scanned only diseased or potentially diseased portions of subtidal leaves for more efficient processing. Consequently, we measured the lengths and widths of each subtidal leaf by hand prior to scanning, and used these to calculate subtidal leaf areas. We scanned entire intertidal leaves, which were smaller than subtidal leaves, and used leaf areas measured by a machine-learning algorithm.

To precisely measure leaf-level disease prevalence and severity, we used the Eelgrass Lesion Image Segmentation Analyzer (EeLISA), a robust algorithm that identified and measured healthy and diseased tissue on all images of scanned eelgrass leaves [9,66,69]. The algorithm calculated disease prevalence (presence/absence of disease) and lesion area for each leaf, along with leaf area estimates for intertidal leaves. Using leaf-level prevalence, which was binary (presence/absence of disease), we calculated transect- and site-level mean prevalence (proportion of surveyed leaves that were infected); we calculated severity (proportion of infected leaf area) using lesion and leaf area measurements at leaf-, transect- and site-levels. Only leaf-level disease prevalence and severity were modelled as response metrics (models detailed below), though transect- and site-level means were useful in understanding and visualizing broad patterns in disease dynamics. For these reasons, we reported leaf-, transect- and site-level disease prevalence and severity. Importantly, this award-winning algorithm was instrumental in enabling us to efficiently and consistently survey disease across a broad, latitudinal scale, as previous methods of measuring disease lesions by hand would have severely limited the scope of our surveys; measuring diseased lesions by hand can take more than 30 min for one eelgrass leaf and can be a significant bottleneck for disease analyses [69]. Furthermore, while desiccation stress presents differently from seagrass wasting disease, which creates characteristic, black lesions [70], discrepancies in human measurements could also lead to lesions being misclassified; EeLISA also helped reduce judgement error.

(c) Pathogen confirmation

We confirmed that the black-edged, necrotic lesions we identified as wasting disease were caused by the pathogen *L. zosterae* and asymptomatic, healthy eelgrass did not contain *L. zosterae* using quantitative polymerase chain reaction (qPCR) ($n = 98$ eelgrass leaves tested), following established protocols [9,28,66,71]. qPCR is a valuable tool for identifying the presence or absence of *L. zosterae* in eelgrass, though it requires precise selection of tissue. Faded, brown lesions from eelgrass in late stages of infection—rather than prominent, dark lesions from new infections—often test negative, as *L. zosterae* has already passed through those plant cells, leaving behind necrotic tissue (M. Eisenlord 2018, personal communication). We used a subset of leaves from British Columbia and Puget Sound surveys for qPCR, specifically targeting intertidal leaves because it was challenging to find large, prominent lesions in subtidal eelgrass. Subsequent qPCR analyses of diseased eelgrass from the San Juan Island, Washington sites also confirmed the presence of *L. zosterae* [66].

(d) Temperature data

To determine the relationship between disease and sea surface temperatures, we assessed remote-sensed sea surface temperatures for all sites from January to June 2017 and 2018, following previously published methods [9,66]. Briefly, we extracted group for high resolution sea surface temperatures (GHRSST) Level 4, multi-scale ultra-high resolution (MUR) daily temperatures for each site from the NASA Jet Propulsion Laboratory OPeNDAP portal, which provides a coherent, consistent daily map of sea surface temperatures at 1 km spatial resolution for each site [72]. The temperature product masked out land using proven algorithms and inputs, and focused on sea surface temperature by combining multi-source satellite data and *in situ* observation records. The specific locations for these 1 km gridded temperatures were based on the GPS coordinates from each site taken during disease surveys. In this way, temperatures were specific to each site, were not measured over the open ocean, and did not differentiate between subtidal and intertidal meadows, as our surveys did not extend beyond a 1 × 1 km area at each site.

To evaluate sea surface temperatures relative to each site, we calculated five different temperature anomaly metrics for each month (from January to June 2017 and 2018, respectively), consistent with previous work exploring impacts of temperature anomalies on marine environments [5,6,66]; we did not use absolute temperatures. All temperature metrics were calculated based on the daily, satellite-derived sea surface temperature for each site and the long-term, 17-year mean (2002–2018) monthly temperature for the site. The five temperature anomaly metrics included: cumulative difference between daily temperature and long-term mean (CDiffMean), cumulative positive difference between daily temperature and long-term mean (CDiffMeanHeat), cumulative negative difference between daily temperature and long-term mean (CDiffMeanCold), cumulative positive difference between daily temperature and long-term 90th percentile monthly temperature (CDiffT90Heat), and cumulative negative difference between daily temperature and long-term 90th percentile monthly temperature (CDiffT90Cold). These temperature anomalies were cumulative temperature differences summed over a one-month period. We restricted temperatures from January to June of 2017 and 2018 since we began our disease surveys in late June of each year, and we did not want to include site temperatures after we had already collected eelgrass. We specifically did not include temperature anomalies for regions sampled after June (Alaska, San Juan Islands, Puget Sound) because we wanted to run temperature anomaly models that compared disease across all regions and sites simultaneously, rather than separate, region-specific models. All temperature metrics from January to June 2017 and January to June 2018 were centred and scaled, then subset by month for subsequent models, described below.

(e) Statistical analyses

We performed all statistical analyses in R v. 4.1.2 [73] and visualized data using the packages ggplot, ggpubr and RcolorBrewer [74–76]. Data exploration and subsequent model fitting and validation were carried out following published protocols [77]. We incorporated remote-sensed sea surface temperatures into models to determine the effects of temperature anomalies and eelgrass biometrics (leaf area, density) on leaf-level disease prevalence and severity. We used the *glmmTMB* function in the glmmTMB package to fit binomial generalized linear mixed

models for prevalence [78], and the *lmer* function and lme4 package to fit linear mixed effects regression models for severity [79]. Fixed effects in all models included tidal zone (subtidal versus intertidal), year, temperature anomaly and leaf area, and interactions (detailed below); subsequent models also included eelgrass density. We centred and scaled all numeric fixed effects—leaf area, density and temperature anomaly—in order for the models to converge. To account for the hierarchical sampling design, we included the random nested effects of region, site, tidal zone and transect in all models. Our nested design allowed for disease comparisons across broad environmental and spatio-temporal gradients.

Given that some parameters were only measured at a subset of sites for both years, we ran several different models on our data. The most comprehensive prevalence and severity models include data from all sites ($n = 5761$ and $n = 3457$ leaves, respectively; electronic supplementary material, table S2). Subsequent prevalence and severity models used a subset of the dataset, which included density ($n = 4090$ and $n = 2549$ leaves; electronic supplementary material, table S3). All data and R scripts used to generate the analyses presented here are publicly available via the Cornell University eCommons Repository (https://doi.org/10.7298/6ybh-w566).

(i) Developing leaf area, temperature and disease models

To determine the best binomial generalized linear mixed model structure for leaf-level prevalence (electronic supplementary material, table S2), we ran models that included fixed effects of leaf area, tidal zone, year, temperature anomaly and interactions between some of these terms (electronic supplementary material, table S2). We only tested interactions that were biologically meaningful, such as leaf area and tidal zone interactions or leaf area and year interactions, but not tidal zone and year interactions. Such interactions were considered potentially biologically meaningful, since subtidal eelgrass leaves are considerably longer and wider compared to those in intertidal zones [80]. Likewise, leaf area could interact with year, if one year was warmer or cooler than another, since temperature strongly influences eelgrass growth [40,41]. We used three temperature anomaly metrics discussed above (CDiffMean, CDiffMeanHeat, CDiffMeanCold) for March in this stage of model development, as March included a range of temperatures above and below the long-term, historical mean. We performed corrected Akaike information criterion (AICc) model selection on these initial candidate models using the *model.sel* function in the R package MuMIn [81] focusing only on March temperature anomalies, to reduce the number of candidate models (electronic supplementary material, table S2). The best-fit, leaf-level prevalence model structure had the lowest AICc and included the following fixed effects and interactions: tidal zone, year, leaf area, temperature anomaly, leaf area*tidal zone, leaf area*year. We then tested this model structure with other temperature anomaly metrics for each month, testing the five different temperature anomaly metrics described above (CDiffMean, CDiffMeanHeat, CDiffMeanCold, CDiffT90Heat, CDiffT90Cold), calculated on a monthly basis from January to June. This allowed us to determine which month's temperature metrics were the best fit for the prevalence model. We again used the MuMIn package to select the best-fit, leaf-level prevalence model (prev mod 1) based on the lowest AICc; this model included a March cold temperature anomaly (CDiffMeanCold, $n = 5761$ leaves; electronic supplementary material, table S2). We validated the model by assessing diagnostic plots (quantile-quantile plots of expected and observed values, model prediction and residual plots) created with the *simulateResiduals* function in the DHARMa package [82].

We followed a similar process to develop the linear mixed effects regression model for leaf-level severity (electronic supplementary material, table S3). Because we used a hurdle model approach for analysing disease severity, we only included data for leaves with disease and excluded healthy individuals; we also logit-transformed severity since the data were bound between 0 and 1, following established protocols [83]. As before, we used the MuMIn package to select the best-fit, leaf-level severity model (sev mod 1) with the lowest AICc [81]; this model included the following fixed effects and interactions: tidal zone, year, leaf area, temperature anomaly and leaf area*temperature anomaly. This severity model included a March cold temperature anomaly (CDiffT90Cold, $n = 3457$ leaves; electronic supplementary material, table S3). To evaluate the model for normality and homogeneity of residuals, we visually checked diagnostic plots created with the *plot_model* function in the sjPlot package [84].

(ii) Developing leaf area, temperature, density and disease models

We developed additional leaf-level prevalence and severity models based on the subset of sites for which we had eelgrass density—British Columbia, San Juan Islands, Puget Sound—following the model development and selection process described above (electronic supplementary material, table S4, tableS5). The best-fit, binomial generalized linear mixed model for leaf-level prevalence (prev mod 2) included the following fixed effects and interactions: tidal zone, year, leaf area, cold temperature anomaly (CDiffMeanCold) for March, density, leaf area*CDiffMeanCold, CDiffMeanCold*mean density, tidal zone*mean density ($n = 4090$ leaves; electronic supplementary material, table S4). The best-fit, linear mixed effects regression hurdle model for leaf-level severity (sev mod 2) included the following fixed effects and interactions: tidal zone, year, leaf area, temperature anomaly (CDiffMean) for March, density, year*CDiffMean ($n = 2549$ leaves; electronic supplementary material, table S5). For this model, we also used a 'bobyqa' optimizer to support model convergence. As before, we used the DHARMa package (*simulateResiduals* function) and the sjPlot package (*plot_model* function) to evaluate diagnostic plots for the prevalence and severity models, respectively [82,84]. For transparency on our model development and selection process, we list all of the prevalence and severity candidate models and their corresponding AICc values in the electronic supplementary materials, tables S2–S5).

3. Results

(a) Broad disease patterns

Disease prevalence and severity were significantly higher in 2018 compared to 2017 when considering data across all sites (prevalence: glmm, $p < 0.001$; electronic supplementary material, table S6; severity: lmer, $p < 0.001$; electronic supplementary material, table S8). Among the four regions, disease prevalence (proportion of infected individual plants) and severity (proportion of tissue infected) increased in all regions in 2018 except for Puget Sound, which had reduced disease (figure 1*b*; electronic supplementary material, figure S2 and table S7). The most dramatic, interannual changes in disease were in the intertidal, particularly in Alaska, where intertidal prevalence increased from 22.05 ± 2.61% to 61.11 ± 3.08% the subsequent year (mean ± s.e.; figure 1*b*; electronic supplementary material, figure S2 and table S7). Intertidal and subtidal meadows in British Columbia and the San Juan Islands also experienced dramatic increases in disease prevalence in 2018, while Puget Sound was anomalous with reduced intertidal and subtidal prevalence in 2018 (electronic supplementary material, table S7). We observed similar, notable increases in severity in 2018 for all regions except Puget Sound (figure 1*b*). Spatially, leaf-level disease prevalence and severity

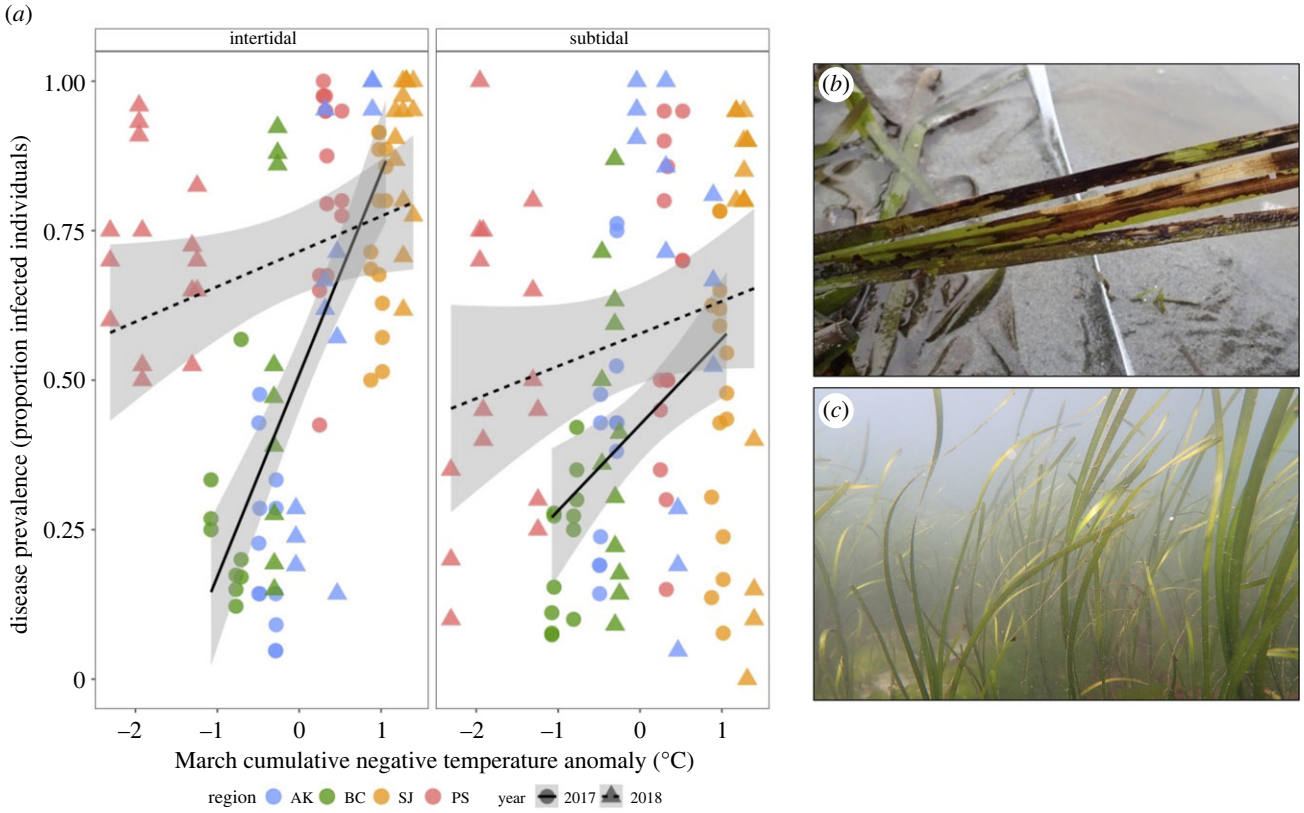

Figure 2. (*a*) Correlations between measured March cumulative negative temperature anomaly and measured transect-level disease prevalence in intertidal and subtidal meadows. Bands represent 95% confidence intervals. Temperature anomalies are centred and scaled. Also shown are representative eelgrass in (*b*) intertidal and (*c*) subtidal meadows. Image (*b*) credit: A. Hausner. AK, southeast Alaska; BC, British Columbia, Canada; SJ, San Juan Islands, Washington; PS, Puget Sound, Washington.

were reduced at higher latitudes compared to lower latitude regions, though disease varied considerably between sites (figure 1*b*; electronic supplementary material, figure S2). This latitudinal gradient was more apparent in the higher-resolution severity data, with Alaska and British Columbia reporting lower disease severity across both years and tidal zones compared to regions further south (figure 1*b*).

Prevalence and severity were significantly lower in subtidal meadows compared to the intertidal (glmm and lmer, $p < 0.001$; electronic supplementary material, table S8). When averaged across both years, the mean prevalence for intertidal eelgrass was 66.0 ± 0.79%, compared to 50.4 ± 1.06% among subtidal plants (mean ± s.e.). At the site-level, disease prevalence ranged from 7.93 ± 3.43% to 100% among intertidal eelgrass and from 8.45 ± 3.32% to 95.23 ± 2.7% among subtidal eelgrass (mean ± s.e.; electronic supplementary material, figure S2). Out of 70 total intertidal and subtidal sampling events across the two years, 41 had a mean prevalence greater than 50%, indicating widespread infection (electronic supplementary material, figure S2). Differences in severity between tidal zones were even more striking (figure 1*b*; electronic supplementary material, table S6). When averaged across both years, severity for intertidal plants was 10.05 ± 0.27%, compared to 3.12 ± 0.17% among subtidal plants (mean ± s.e.). Site-level disease severity ranged from 0.14 ± 0.096% to 33 ± 1.85% among intertidal eelgrass, compared to 0.054 ± 0.029% to 16.3 ± 2.78% among subtidal eelgrass (mean ± s.e.; figure 1*b*).

(b) Leaf area, temperature and disease models

We tested five temperature metrics calculated for each month (January–June) when developing leaf-level prevalence and severity models. Of these, March temperature anomalies were in the best-fit models, based on the lowest AICc (electronic supplementary material, table S6). Sea surface temperatures in March 2017 and 2018 varied regionally, with generally colder absolute temperatures in higher-latitude regions (electronic supplementary material, figure S3). All regions experienced warmer temperatures in March 2018 than March 2017 except for Puget Sound, which was cooler that year (electronic supplementary material, figure S4). This coincided with reduced disease prevalence and severity in Puget Sound relative to 2017 (figure 1*b*; electronic supplementary material, figure S2).

Leaf-level, prevalence significantly decreased with cooler March temperatures, as predicted (glmm, $p < 0.001$; electronic supplementary material, table S6). Predicted prevalence decreased with cooler March temperature anomalies (CDiffMeanCold) for both intertidal and subtidal eelgrass (electronic supplementary material, figure S4). Other significant predictors for leaf-level prevalence included: tidal zone, year, leaf area, leaf area*tidal zone and leaf area*year (glmm, $p < 0.001$; electronic supplementary material, table S6). Across both tidal zones, transect-level disease prevalence was positively associated with cumulative March cold temperature anomalies (CDiffMeanCold) and leaf areas (figure 2*a*; electronic supplementary material, figure S6).

Similarly, leaf-level severity significantly decreased with cooler March temperatures (lmer, $p < 0.001$; electronic supplementary material, table S6). Among diseased leaves, predicted severity decreased with cumulative, 90th percentile cold March temperature anomalies in subtidal and intertidal eelgrass (electronic supplementary material, figure S5). Compared to absolute cold temperature anomalies measured on a daily basis, this cold temperature anomaly (CDiffT90Cold) is

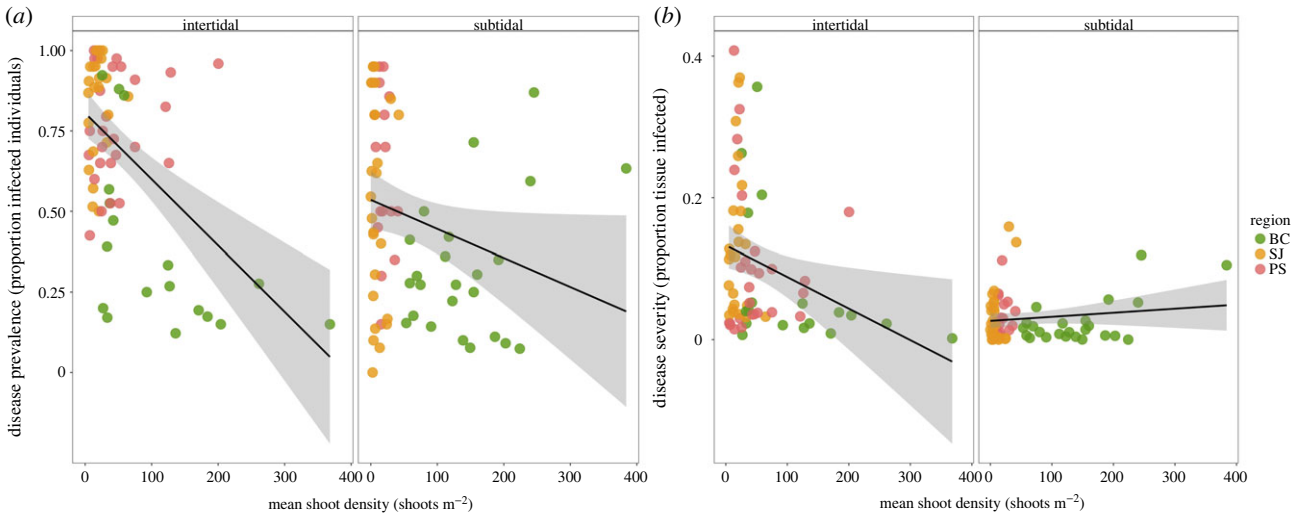

Figure 3. Transect-level mean wasting disease (*a*) prevalence and (*b*) severity in response to eelgrass density in intertidal and subtidal eelgrass. Bands represent 95% confidence intervals. AK, southeast Alaska; BC, British Columbia, Canada; SJ, San Juan Islands, Washington; PS, Puget Sound, Washington.

the accumulation of negative differences between each site's daily temperatures and the long-term 90th percentile mean temperatures for March 2017 and 2018. Other significant predictors of leaf-level severity include tidal zone, year and leaf area*CDiffT90Cold (lmer, $p < 0.001$; electronic supplementary material, table S6). For intertidal leaves, disease severity was positively associated with cumulative, 90th percentile March cold temperature anomalies and leaf areas, though these associations were not as apparent among subtidal leaves (electronic supplementary material, figures S6 and S7).

(c) Leaf area, temperature, density and disease models

Mean eelgrass densities varied among sites and tidal zones and between years for several sites (electronic supplementary material, figure S8). Shoot densities were significantly higher in intertidal meadows compared to subtidal in the San Juan Islands (*t*-test: $t_{178} = 4.01$, $p < 0.001$) and Puget Sound ($t_{103} = 2.60$, $p = 0.01$), but not in British Columbia (electronic supplementary material, figure S8; $t_{124} = -1.82$, $p = 0.07$). At the transect level, low-density intertidal and subtidal eelgrass had higher disease prevalence and severity compared to eelgrass at higher densities (figure 3). Changes in mean density in 2018 were not strongly associated with the prior year mean severity (data not shown), suggesting that other factors probably interact with disease to influence eelgrass persistence.

Leaf-level prevalence was significantly, inversely associated with mean shoot density (glmm, $p < 0.001$; electronic supplementary material, table S8). High disease levels were associated with reduced eelgrass densities in both subtidal and intertidal meadows (figure 3). The best-fit prevalence and density model included the following predictors, all of which were significant: tidal zone, leaf area, year, March cold temperature anomaly (CDiffMeanCold), density, leaf area*CDiffMeanCold, CDiffMeanCold*density, tidal zone*density (electronic supplementary material, table S8). Interactions between temperature and density had the most pronounced effect on predicted prevalence at low densities. At low densities, lower predicted disease prevalence was associated with cooler temperatures, while higher predicted prevalence was associated with warmer temperatures (electronic supplementary material, figure S9). This association was consistent at mean densities, but did not persist at high eelgrass densities.

Leaf-level severity was not significantly associated with mean shoot density (lmer, $p > 0.05$; electronic supplementary material, table S8). The best-fit, hurdle severity model included the following: tidal zone, leaf area, year, March temperature anomaly (CDiffMean), density, year*CDiffMean. There was not a consistent association between March temperature anomaly, eelgrass densities, and predicted severity in 2017 and 2018 (data not shown).

(d) Eelgrass biometrics

Consistent with previous work [80], eelgrass leaves were smaller at shallower depths (electronic supplementary material, figure S8). Mean canopy height was 599.02 mm ± 9.99% in intertidal eelgrass and 1068.71 mm ± 14.58% in subtidal eelgrass when averaged across years (mean ± s.e.; electronic supplementary material, figure S8). Mean leaf area was also smaller among intertidal eelgrass compared to subtidal eelgrass. Across both years, mean leaf area was 1935.14 mm^2 ± 24.31% in intertidal eelgrass and 5267.93 mm^2 ± 72.76% in subtidal eelgrass (mean ± s.e.; electronic supplementary material, figure S8). Leaf area was significantly, positively associated with leaf-level disease prevalence (glmm, $p < 0.001$; electronic supplementary material, table S6). Although subtidal eelgrass leaves were on average nearly three times larger than intertidal eelgrass, disease prevalence and severity were significantly lower in subtidal plants.

(e) Quantitative polymerase chain reaction

We successfully confirmed the presence of *L. zosterae* in 19 out of 49 symptomatic, lesioned eelgrass from British Columbia and Puget Sound using qPCR. It is possible that we may have tested both new and old infections, leading to this 38.7% positive rate. These results are comparable to other studies that confirmed *L. zosterae* in diseased eelgrass in the San Juan Islands and Alaska [9,29,30,53,66,85]. All asymptomatic eelgrass tested from these regions were qPCR negative for the pathogen ($n = 49$). We isolated *L. zosterae* from diseased eelgrass in the San Juan Islands to confirm pathogen

presence (data not shown). Overall, these findings support that our visual identification of lesions were caused by *L. zosterae*.

4. Discussion

The two study years, 2017 and 2018, captured outbreak conditions of relatively high disease levels across a wide latitude in the northern range of eelgrass, from Puget Sound to Alaska, including some relatively undisturbed, remote locations. Our observed disease prevalence and severity levels are comparable to those documented in other intertidal and subtidal eelgrass meadows in the northeast Pacific [66], including the San Juan Islands [9,51,66], though severity levels are considerably higher than those observed in Sweden [31]. Previous work indicates that in natural meadows, growth rates and belowground sugar reserves are reduced in diseased eelgrass and lesions can rapidly outpace leaf growth [20]. Thus, eelgrass growth appears compromised—and potentially survival—in meadows with high disease. Against this backdrop of high disease levels, disease risk varied highly across both latitude and tidal zone. Cooler sites, the cooler year and higher latitudes had reduced disease prevalence and severity. This suggests seagrass wasting disease is among the growing number of temperature-sensitive marine diseases [5,10,66].

Of the temperature metrics tested in prevalence and severity models, March cold temperature anomalies were the best predictors for summertime disease levels. Regions with cooler temperatures that may either kill or slow the growth of *L. zosterae* could have lower summer disease levels. In pure culture, *L. zosterae* has a lower thermal limit of 0°C [52]. While most regions experienced cooler temperatures and reduced disease in 2017, the exception was a cooler Puget Sound in 2018, which stood out as reflecting a temperature-disease association. Disease prevalence and severity were markedly lower in Puget Sound that year, coinciding with cooler La Niña conditions—including increased upwelling—that provided more cool, saline water to the area in spring 2018 [86]. This local anomaly in cooler temperatures and lower disease further supports the notion that cooler temperatures suppress disease. By contrast, warmer spring temperatures could allow the pathogen to proliferate, causing disease outbreaks by the summer. Similar associations between June positive temperature anomalies and elevated disease were recently observed in intertidal eelgrass in the northeast Pacific [66]. Based on these findings, spring temperatures could serve as an early indicator for summertime disease outbreaks. However, because cold temperatures help control wasting disease, future warming conditions could provide more favourable environments for *L. zosterae*, threatening the sustainability of infected eelgrass meadows.

Other factors probably influence wasting disease dynamics, such as light and salinity (reviewed in [14]). Light is a key driver of eelgrass growth and survival, limiting their lower depth limits [87]. Simulation experiments predicted that poorly illuminated growing conditions in the 1930s would have killed eelgrass meadows in the Dutch Wadden Sea, regardless of the raging wasting disease outbreaks at that time [88]. In our study, northern latitude sites with longer day length may have had better growing conditions for eelgrass, enabling plants to suppress infection. This could, in part, account for the overall reduced disease prevalence and severity observed at higher latitudes. Laboratory experiments also reflect an inverse association between light and wasting disease, as mean severity was 35% higher in eelgrass grown under reduced light compared to eelgrass under ambient light [89]. Light can interact with other stressors like temperature, which can alter the photosynthesis capabilities of eelgrass leaves [90], further compromising eelgrass health.

Associations between salinity and seagrass wasting disease were detected in previous studies. Wasting disease was not detected in Swedish low salinity meadows (13–25 practical salinity units (PSU)), but it was present at all high salinity meadows (25–29 PSU) [31]. In laboratory studies, eelgrass exposed to lower salinities developed smaller lesions [70,91]; *L. zosterae* also had reduced reproductive rates under low salinity conditions [17,50,70,92]. While all of our survey sites were marine, they probably spanned a range of salinities, given the proximity of some sites to freshwater sources (e.g. Fraser River in British Columbia). Though we did not include salinity in these analyses, future studies would benefit from including *in situ* or modelled salinity measurements [93]. This association between reduced salinity and wasting disease is especially compelling, as low salinity meadows could serve as refuge from disease. Given that many stressors independently and synergistically favour *L. zosterae*, future studies should explore how multiple stressors influence seagrass wasting disease dynamics in laboratory conditions and natural meadows [89]. This project adds an important line of evidence on the role of ocean temperatures.

Sites spanned environmental and latitudinal gradients, allowing us to measure disease across a broad spatial scale. Our results indicate widespread disease prevalence across all sites, and suggest that sites with severe infections could be at risk for future declines. Further, they indicate that even remote meadows with minimal human impacts, like Alaska and British Columbia, are at risk for disease outbreaks. Since high-latitude meadows had lower disease compared to those at lower latitudes—and given that eelgrass ranges are expected to expand northwards under climate change scenarios [47]—these northern meadows should be carefully monitored as potential refugia against disease and warm temperatures. A number of factors were confounded with geographical region, including timing of sampling, latitude, salinity, and human impacts (e.g. coastal development, water quality). While our study design could not partition the variation associated with these factors, they may be important in influencing wasting disease dynamics. For example, coastal urbanization could compromise eelgrass health, since nutrient enrichment from runoff triggers algal blooms and suspended sediments limit light, stressors that caused seagrass loss in an urban Florida estuary [94]. Future work should target multiple wasting disease stressors.

Across regions and years, subtidal meadows had significantly lower disease prevalence and severity than intertidal meadows. When averaged across both years, subtidal meadows had nearly three times lower disease severity, suggesting deeper habitats buffered the effects of environmental stressors and disease. Subtidal eelgrass may be more resilient and thus more resistant to wasting disease compared to intertidal eelgrass, and these deeper meadows could serve as refugia from future disease outbreaks and climate change conditions. This is consistent with findings that 20 years after mass eelgrass die-offs in the Chausey Archipelago, France, recovery was mostly

limited to subtidal meadows [95]. Similar to terrestrial plants in environmental extremes [96], intertidal eelgrass that is exposed to highly variable environmental conditions at low tide—high and low temperatures, salinity, desiccation, UV stress [64]—may be more physiologically stressed and at risk to infection compared to subtidal meadows, which are not exposed at low tide and may be more disease resilient. Similarly, deep temperate reefs act as refugia against marine heatwaves for habitat-forming corals, seaweeds, and eelgrass in Virginia and the northeast Pacific, buffering against the harsh environmental conditions to which organisms at shallower depths are exposed [46,60–62,97]. At the same time, compromised light conditions owing to eutrophication and sediment inputs from coastal development could moderate this subtidal refugia effect. Subtidal meadows already experience reduced light levels compared to shallower, intertidal eelgrass [87]; these differences are exacerbated in areas with poor water quality, which should be carefully monitored for disease and overall eelgrass health.

Sites with denser eelgrass meadows and cooler temperatures had lower disease, regardless of tidal zone, but this association was more pronounced in intertidal meadows. However, this pattern is contrary to our hypothesis and disease theory, which would predict higher disease levels in denser meadows, given that one of the mechanisms of seagrass wasting disease transmission is via direct contact between infected and healthy leaves [15]. Meadows with low eelgrass densities could have already experienced disease outbreaks or stressful conditions, leaving a reduced number of survivors with high disease prevalence and severity. Given that we observed higher disease levels in patchier meadows and strong interactions between temperature and density on disease prevalence, patchy meadows are probably more at risk to synergies between thermal and disease stressors. Recent work corroborates similar findings on the resiliency of deeper eelgrass habitats, which had positive or neutral changes in density following a marine heatwave, compared to significant declines in warmer, shallower meadows [46]. As such, high density eelgrass meadows under lower climate stress should be prioritized for conservation.

Generally, the mean densities, canopy heights, and leaf areas we observed were comparable to those in other eelgrass meadows in the northeast Pacific [9,30,66]. Across all regions, the greater canopy heights and leaf areas observed in subtidal eelgrass compared to intertidal eelgrass are consistent with established differences in eelgrass growth patterns between tidal zones [80,98]. Intertidal and subtidal densities varied considerably, with orders of magnitude higher densities occurring at some sites compared to others in the same tidal zone. Densities were more consistent in subtidal meadows year to year than intertidal meadows. This is consistent with seasonal comparisons of intertidal and subtidal eelgrass meadows in Ireland, where subtidal meadows had a smaller range of seasonal shoot densities compared to intertidal eelgrass [80]. Collectively, these results further support our hypothesis that subtidal meadows are more environmentally stable and resilient against environmental disturbances; this is also reflected in lower disease in subtidal meadows. Our findings that leaf area and disease prevalence were significantly, positively associated also aligns with previous findings [9,29,30]. Based on leaf area alone and the usual association between disease and leaf size, subtidal meadows should have more disease, yet subtidal meadows consistently had reduced prevalence and severity. Again, this suggests greater resilience to disease of deeper, natural eelgrass meadows.

We specifically designed surveys to determine the association between temperature and disease in natural eelgrass meadows spanning the high biodiversity northeast Pacific. Temperature is an important driver of historic and current wasting disease outbreaks worldwide [9,13,14,27,66,99]. Our machine-learning algorithm, EeLISA, enabled us to prioritize precise, repeatable disease assignments and scale up our surveys. Field surveys that span broad, spatio-temporal scales are essential to tracking and predicting disease outbreaks in a rapidly changing ocean, and are needed to inform conservation and management decisions [100–102].

Connecting across scales from individuals, tidal zones, sites and geographical regions, this large-scale field survey furthers our understanding of seagrass wasting disease dynamics in a changing ocean. Notably, it shows an association between reduced eelgrass disease, cooler temperatures, higher eelgrass densities and deeper habitats. Our findings underscore a central need in managing marine resources in a rapidly warming climate: mapping resilient refugia. Surveys also reveal the conservation value of subtidal meadows, which are largely out of sight. This new indication of important refuge from climate stressors and disease significantly increases the value of subtidal meadows, many of which are declining within the Salish Sea [9,51,68] and globally [39]. While previous field surveys compared wasting disease in eelgrass at different intertidal [9,29] and subtidal zones [31], to our knowledge, no prior studies have compared disease between tidal zones. A relatively understudied aspect of wasting disease in eelgrass, these deeper refugia provide important opportunities for future conservation efforts.

This new information about lower wasting disease risk in cooler climates, cooler years, and deeper meadows can improve eelgrass management. First, to best inform conservation and preservation of these key habitats under mounting climate stress, continued monitoring of eelgrass meadows is essential, especially to gauge and track temperature-sensitive disease outbreaks. Intertidal meadows are most tractable for disease surveys, since they not only are easier to access from shore, but also have higher levels of disease, are more at risk, and may provide earlier warning of declines. Second, more protections should also be considered for both intertidal and subtidal meadows to buffer against future climate and disease-driven declines, especially in areas prone to more frequent, rapid warming and compromised water quality, as these meadows have higher risk for disease outbreaks. Because subtidal meadows have the highest potential as safe havens against environmental and pathogenic stressors, eelgrass conservation activities should focus on protecting subtidal meadows. Given the increasing frequency and intensity of marine heatwaves [36,103], other mounting environmental changes, and global seagrass declines [39], understanding the synergistic effects of climate change and marine diseases on this foundation species is critical to the sustainability of our oceans and planet [7].

Data accessibility. All data and R scripts used to generate the analyses presented here are publicly available via the Cornell University eCommons Repository (https://doi.org/10.7298/6ybh-w566) [104].

Additional figures, tables, and a video are provided in the electronic supplementary material [105].

Authors' contributions. O.J.G.: conceptualization, data curation, formal analysis, funding acquisition, investigation, methodology, project

administration, resources, supervision, validation, visualization, writing—original draft, writing—review and editing; T.S.: investigation, project administration, writing—review and editing; B.R.: formal analysis, investigation, methodology, resources, software, writing—review and editing; C.K.: investigation, software, writing—review and editing; S.D.: investigation, writing—review and editing; E.M.A.: investigation, writing—review and editing; A.O.: investigation, writing—review and editing; M.H.-L.: investigation, project administration, resources, supervision, writing—review and editing; M.E.: investigation, writing—review and editing; B.Y.: investigation, resources, writing—review and editing; C.B.: investigation, resources, writing—review and editing; C.P.G.: conceptualization, funding acquisition, investigation, project administration, resources, software, supervision, writing—review and editing; D.H.: conceptualization, funding acquisition, investigation, project administration, resources, supervision, writing—original draft, writing—review and editing.

All authors gave final approval for publication and agreed to be held accountable for the work performed therein.

Conflict of interest declaration. We declare we have no competing interests.

Funding. The following generous funds supported this work: Cornell University's Atkinson Center for Sustainable Biodiversity Fund, Cornell Engaged Graduate Student Grant, Cornell Sigma Xi Research Grant, Andrew W. Mellon Student Research Grant, Dr Carolyn Haugen, University of Washington Friday Harbor Labs Graduate Research Fellowship Endowment, Women Diver's Hall of Fame Scholarship in Marine Conservation to O.J.G.; NSF-REU and Susan Lynch support for the Cornell Ocean Research Apprenticeship for Lynch Scholars to C.K. and S.D.; NSF awards OCE-1829921 and Washington SeaGrant (grant no. NA18OAR4170095) to C.B., Carolyn Friedman, CDH; NSF CompSustNet: Expanding the Horizons of Computational Sustainability (grant no. 1522054) to C.G.; Tula Foundation to O.J.G., E.M.A., A.O., M.H.-L.

Acknowledgements. We would like to thank our dedicated field research assistants who supported this project: Phoebe Dawkins, Coco Dawkins, James Lee, Miranda Winningham, Jack Novack, Carolyn Prentice, Tanya Prinzing, John Cristiani, Zach Monteith, Willem Weertman, Alex Lowe, Joey Ullman, Abigail Ames, Julia Kobelt, Christopher Wells, Maggie Shields, and Wendel Raymond. We would also like to thank Willem Weertman for making the ArcGIS map. Special thanks to Lillian Aoki, Maya Groner, Lynn Johnson, and Erika Mudrak for their invaluable statistical advice. Thanks to Nick Tolimieri for his instrumental support with Puget Sound fieldwork in summer 2017. Finally, we would like to thank anonymous reviewers for their supportive, constructive feedback.

References

1. Harvell CD, Mitchell C, Ward J, Altizer S, Dobson A, Ostfeld R, Samuel M. 2002 Climate warming and disease risks for terrestrial and marine biota. *Science* **296**, 2158–2162. (doi:10.1126/science.1063699)
2. Ward JR, Lafferty KD. 2004 The elusive baseline of marine disease: are diseases in ocean ecosystems increasing? *PLoS Biol.* **2**, e120. (doi:10.1371/journal.pbio.0020120)
3. Tracy AM, Pielmeier ML, Yoshioka RM, Heron SF, Harvell CD. 2019 Increases and decreases in marine disease reports in an era of global change. *Proc. R. Soc. B* **286**, 20191718. (doi:10.1098/rspb.2019.1718)
4. Harvell CD. 1999 Emerging marine diseases–climate links and anthropogenic factors. *Science* **285**, 1505–1510. (doi:10.1126/science.285.5433.1505)
5. Harvell CD *et al.* 2019 Disease epidemic and a marine heat wave are associated with the continental-scale collapse of a pivotal predator (*Pycnopodia helianthoides*). *Sci. Adv.* **5**, eaau7042. (doi:10.1126/sciadv.aau7042)
6. Hobday AJ *et al.* 2016 A hierarchical approach to defining marine heatwaves. *Prog. Oceanogr.* **141**, 227–238. (doi:10.1016/j.pocean.2015.12.014)
7. Burge CA, Hershberger PK. 2020 Climate change can drive marine diseases. In *Marine disease ecology* (eds DC Behringer, BR Silliman, KD Lafferty), pp. 83–94. Oxford, UK: Oxford University Press.
8. Strydom S *et al.* 2020 Too hot to handle: unprecedented seagrass death driven by marine heatwave in a World Heritage Area. *Glob. Change Biol.* **26**, 3525–3538. (doi:10.1111/gcb.15065)
9. Groner M *et al.* 2021 Warming sea surface temperatures fuel summer epidemics of eelgrass wasting disease. *Mar. Ecol. Prog. Ser.* **679**, 47–58. (doi:10.3354/meps13902))
10. Caldwell J, Heron S, Eakin C, Donahue M. 2016 Satellite SST-based coral disease outbreak predictions for the Hawaiian Archipelago. *Remote Sens.* **8**, 93. (doi:10.3390/rs8020093)
11. Harvell CD, Lamb JB. 2020 Disease outbreaks can threaten marine biodiversity. In *Marine disease ecology* (eds DC Behringer, BR Silliman, KD Lafferty), pp. 141–158. Oxford, UK: Oxford University Press.
12. Green E, Short F (eds) In press. *World atlas of seagrasses*. Berkeley, CA: University of California Press.
13. Martin DL, Chiari Y, Boone E, Sherman TD, Ross C, Wyllie-Echeverria S, Gaydos JK, Boettcher AA. 2016 Functional, phylogenetic and host-geographic signatures of labyrinthula spp. provide for putative species delimitation and a global-scale view of seagrass wasting disease. *Estuaries Coasts* **39**, 1403–1421. (doi:10.1007/s12237-016-0087-z)
14. Sullivan BK, Trevathan-Tackett SM, Neuhauser S, Govers LL. 2018 Review: host-pathogen dynamics of seagrass diseases under future global change. *Mar. Pollut. Bull.* **134**, 75–88. (doi:10.1016/j.marpolbul.2017.09.030)
15. Muehlstein LK. 1992 The host – pathogen interaction in the wasting disease of eelgrass, *Zostera marina*. *Can. J. Bot.* **70**, 2081–2088. (doi:10.1139/b92-258)
16. Ralph P, Short F. 2002 Impact of the wasting disease pathogen, Labyrinthula zosterae, on the photobiology of eelgrass *Zostera marina*. *Mar. Ecol. Prog. Ser.* **226**, 265–271. (doi:10.3354/meps226265)
17. Pokorny KS. 1967 *Labyrinthula*. *J. Protozool.* **14**, 697–708. (doi:10.1111/j.1550-7408.1967.tb02065.x)
18. Short F, Mathieson A, Nelson J. 1986 Recurrence of the eelgrass wasting disease at the border of New Hampshire and Maine, USA. *Mar. Ecol. Prog. Ser.* **29**, 89–92. (doi:10.3354/meps029089)
19. Burdick D, Short F, Wolf J. 1993 An index to assess and monitor the progression of wasting disease in eelgrass *Zostera marina*. *Mar. Ecol. Prog. Ser.* **94**, 83–90. (doi:10.3354/meps094083)
20. Graham OJ, Aoki LR, Stephens T, Stokes J, Dayal S, Rappazzo B, Gomes CP, Harvell CD. 2021 Effects of seagrass wasting disease on eelgrass growth and belowground sugar in natural meadows. *Front. Mar. Sci.* **8**, 768668. (doi:10.3389/fmars.2021.768668)
21. Renn C. 1936 The wasting disease of *Zostera marina*: a phytological investigation of the diseased plant. *Biol. Bull.* **70**, 148–158.
22. Short FT, Ibelings BW, Den Hartog C. 1988 Comparison of a current eelgrass disease to the wasting disease in the 1930s. *Aquat. Bot.* **30**, 295–304. (doi:10.1016/0304-3770(88)90062-9)
23. Stauffer RC. 1937 Changes in the invertebrate community of a lagoon after disapperance of the eel grass. *Ecology* **18**, 427–431. (doi:10.2307/1931212)
24. Moffitt J, Cottam C. 1941 Eelgrass depletion on the Pacific coast and its effect upon the Black Brant. US Department of the Interior, Report 204:26.
25. Milne L, Milne M. 1951 The eelgrass catastrophe. *Sci. Am.* **184**, 52–55.
26. Rasmussen E. 1977 The wasting disease of eelgrass (*Zostera marina*) and its effects on environmental factors and fauna. In *Seagrass ecosystems: a scientific perspective* (eds CP McRoy, C Helfferich), pp. 1–52. New York, NY: Marcel Dekker.
27. Bull JC, Kenyon EJ, Cook KJ. 2012 Wasting disease regulates long-term population dynamics in a threatened seagrass. *Oecologia* **169**, 135–142. (doi:10.1007/s00442-011-2187-6)
28. Bockelmann A-C, Tams V, Ploog J, Schubert PR, Reusch TBH. 2013 Quantitative PCR reveals strong spatial and temporal variation of the wasting disease pathogen, *Labyrinthula zosterae* in northern European eelgrass (*Zostera marina*) beds. *PLoS ONE* **8**, e62169. (doi:10.1371/journal.pone.0062169)

29. Groner M *et al.* 2014 Host demography influences the prevalence and severity of eelgrass wasting disease. *Dis. Aquat. Organ.* **108**, 165–175. (doi:10.3354/dao02709)
30. Groner M, Burge C, Kim C, Rees E, Van Alstyne K, Yang S, Wyllie-Echeverria S, Harvell C. 2016 Plant characteristics associated with widespread variation in eelgrass wasting disease. *Dis. Aquat. Organ.* **118**, 159–168. (doi:10.3354/dao02962)
31. Jakobsson-Thor S, Toth G, Brakel J, Bockelmann A, Pavia H. 2018 Seagrass wasting disease varies with salinity and depth in natural *Zostera marina* populations. *Mar. Ecol. Prog. Ser.* **587**, 105–115. (doi:10.3354/meps12406)
32. Aoki LR *et al.* 2022 Disease surveillance by artificial intelligence links eelgrass wasting disease to ocean warming across latitudes. *Limnol. Oceanogr.* **67**, 1577–1589. (doi:10.1002/lno.12152)
33. Bos AR, Bouma TJ, de Kort GLJ, van Katwijk MM. 2007 Ecosystem engineering by annual intertidal seagrass beds: sediment accretion and modification. *Estuar. Coast. Shelf Sci.* **74**, 344–348. (doi:10.1016/j.ecss.2007.04.006)
34. Schmidt AL, Wysmyk JKC, Craig SE, Lotze HK. 2012 Regional-scale effects of eutrophication on ecosystem structure and services of seagrass beds. *Limnol. Oceanogr.* **57**, 1389–1402. (doi:10.4319/lo.2012.57.5.1389)
35. Prentice C *et al.* 2020 A synthesis of blue carbon stocks, sources, and accumulation rates in eelgrass (*Zostera marina*) meadows in the northeast Pacific. *Glob. Biogeochem. Cycles* **34**, e2019GB006345. (doi:10.1029/2019GB006345)
36. Oliver ECJ *et al.* 2018 Longer and more frequent marine heatwaves over the past century. *Nat. Commun.* **9**, 1324. (doi:10.1038/s41467-018-03732-9)
37. Short FT, Kosten S, Morgan PA, Malone S, Moore GE. 2016 Impacts of climate change on submerged and emergent wetland plants. *Aquat. Bot.* **135**, 3–17. (doi:10.1016/j.aquabot.2016.06.006)
38. Smale DA *et al.* 2019 Marine heatwaves threaten global biodiversity and the provision of ecosystem services. *Nat. Clim. Change* **9**, 306–312. (doi:10.1038/s41558-019-0412-1)
39. Dunic JC, Brown CJ, Connolly RM, Turschwell MP, Côté IM. 2021 Long-term declines and recovery of meadow area across the world's seagrass bioregions. *Glob. Change Biol.* **27**, 4096–4109. (doi:10.1111/gcb.15684)
40. Kaldy JE. 2014 Effect of temperature and nutrient manipulations on eelgrass *Zostera marina* L. from the Pacific northwest, USA. *J. Exp. Mar. Biol. Ecol.* **453**, 108–115. (doi:10.1016/j.jembe.2013.12.020)
41. Thom R, Southard S, Borde A. 2014 Climate-linked mechanisms driving spatial and temporal variation in eelgrass (*Zostera marina* L.) growth and assemblage structure in Pacific northwest estuaries, U.S.A. *J. Coast. Res.* **68**, 1–11. (doi:10.2112/SI68-001.1)
42. Moore KA, Shields EC, Parrish DB. 2014 Impacts of varying estuarine temperature and light conditions on *Zostera marina* (eelgrass) and its interactions with *Ruppia maritima* (widgeongrass). *Estuaries Coasts* **37**, 20–30. (doi:10.1007/s12237-013-9667-3)
43. Ehlers A, Worm B, Reusch TBH. 2008 Importance of genetic diversity in eelgrass *Zostera marina* for its resilience to global warming. *Mar. Ecol. Prog. Ser.* **355**, 1–7. (doi:10.3354/meps07369)
44. Bintz JC, Nixon SW, Buckley BA, Granger SL. 2003 Impacts of temperature and nutrients on coastal lagoon plant communities. *Estuaries* **26**, 765. (doi:10.1007/BF02711987)
45. Kendrick GA *et al.* 2019 A systematic review of how multiple stressors from an extreme event drove ecosystem-wide loss of resilience in an iconic seagrass community. *Front. Mar. Sci.* **6**, 455. (doi:10.3389/fmars.2019.00455)
46. Magel CL, Chan F, Hessing-Lewis M, Hacker SD. 2022 Differential responses of eelgrass and macroalgae in Pacific northwest estuaries following an unprecedented NE Pacific Ocean marine heatwave. *Front. Mar. Sci.* **9**, 838967. (doi:10.3389/fmars.2022.838967)
47. Wilson K, Lotze H. 2019 Climate change projections reveal range shifts of eelgrass *Zostera marina* in the northwest Atlantic. *Mar. Ecol. Prog. Ser.* **620**, 47–62. (doi:10.3354/meps12973)
48. Orth RJ *et al.* 2006 A global crisis for seagrass ecosystems. *BioScience* **56**, 987. (doi:10.1641/0006-3568(2006)56[987:AGCFSE]2.0.CO;2)
49. Stevens NE. 1936 Environmental conditions and the wasting disease of eel-grass. *Science* **84**, 87–89. (doi:10.1126/science.84.2169.87)
50. Young E. 1943 Studies on *Labyrinthula*, the etiologic agent of the wasting disease of eel-grass. *Am. J. Bot.* **30**, 586–593.
51. Aoki LR, Yang B, Graham OJ, Gomes GC, Rappazzo B, Hawthorne TL, Duffy JE, Harvell D. 2023 UAV high-resolution imaging and disease surveys combine to quantify climate-related decline in seagrass meadows. In *Frontiers in Ocean Observing: emerging Technologies for Understanding and Managing a Changing Ocean* (eds ES Kappel, V Cullen, MJ Costello, L Galgani, C Gordó-Vilaseca, A Govindarajan, S Kouhi, C Lavin, L McCartin, JD Müller, B Pirenne, T Tanhua, Q Zhao, S Zhao). *Oceanography* **36**(Suppl. 1). (https://doi.org/10.5670/oceanog.2023.s1.12).
52. Amon J. 1968 Studies of *Labyrinthula* spp in culture, p. 21. MA thesis, College of William and Mary, Williamsburg, VA, USA. See https://scholarworks.wm.edu/etd/1539617410/.
53. Dawkins P, Eisenlord M, Yoshioka R, Fiorenza E, Fruchter S, Giammona F, Winningham M, Harvell C. 2018 Environment, dosage, and pathogen isolate moderate virulence in eelgrass wasting disease. *Dis. Aquat. Organ.* **130**, 51–63. (doi:10.3354/dao03263)
54. Burge CA, Kim CJS, Lyles JM, Harvell CD. 2013 Special issue oceans and humans health: the ecology of marine opportunists. *Microb. Ecol.* **65**, 869–879. (doi:10.1007/s00248-013-0190-7)
55. Dennison WC, Alberte RS. 1982 Photosynthetic responses of *Zostera marina* L. (eelgrass) to in situ manipulations of light intensity. *Oecologia* **55**, 137–144. (doi:10.1007/BF00384478)
56. Koch EW. 2001 Beyond light: physical, geological, and geochemical parameters as possible submersed aquatic vegetation habitat requirements. *Estuaries* **24**, 1. (doi:10.2307/1352808)
57. Keppel G, Wardell-Johnson GW. 2012 Refugia: keys to climate change management. *Glob. Change Biol.* **18**, 2389–2391. (doi:10.1111/j.1365-2486.2012.02729.x)
58. Keppel G, Van Niel KP, Wardell-Johnson GW, Yates CJ, Byrne M, Mucina L, Schut AGT, Hopper SD, Franklin SE. 2012 Refugia: identifying and understanding safe havens for biodiversity under climate change: Identifying and understanding refugia. *Glob. Ecol. Biogeogr.* **21**, 393–404. (doi:10.1111/j.1466-8238.2011.00686.x)
59. Ellertsdottir E, Peters A. 1997 High prevalence of infection by endophytic brown algae in populations of *Laminaria* spp (Phaeophyceae). *Mar. Ecol. Prog. Ser.* **146**, 135–143.
60. Ladah LB, Zertuche-González JA. 2004 Giant kelp (*Macrocystis pyrifera*) survival in deep water (25–40 m) during El Niño of 1997–1998 in Baja California, Mexico. *Botanica Marina* **47**, 367–372. (doi:10.1515/BOT.2004.054)
61. Van Oppen MJH, Bongaerts P, Underwood JN, Peplow LM, Cooper TF. 2011 The role of deep reefs in shallow reef recovery: an assessment of vertical connectivity in a brooding coral from west and east Australia. *Mol. Ecol.* **20**, 1647–1660. (doi:10.1111/j.1365-294X.2011.05050.x)
62. Giraldo-Ospina A, Kendrick GA, Hovey RK. 2020 Depth moderates loss of marine foundation species after an extreme marine heatwave: could deep temperate reefs act as a refuge? *Proc. R. Soc. B* **287**, 20200709. (doi:10.1098/rspb.2020.0709)
63. Robertson AI, Mann KH. 1984 Disturbance by ice and life-history adaptations of the seagrass *Zostera marina*. *Mar. Biol.* **80**, 131–141. (doi:10.1007/BF02180180)
64. Park SR, Kim S, Kim YK, Kang C-K, Lee K-S. 2016 Photoacclimatory responses of *Zostera marina* in the intertidal and subtidal zones. *PLoS ONE* **11**, e0156214. (doi:10.1371/journal.pone.0156214)
65. Zamora-Vilchis I, Williams SE, Johnson CN. 2012 Environmental temperature affects prevalence of blood parasites of birds on an elevation gradient: implications for disease in a warming climate. *PLoS ONE* **7**, e39208. (doi:10.1371/journal.pone.0039208)
66. Aoki L et al. 2022 Disease surveillance by artificial intelligence links seagrass wasting disease to ocean warming across latitudes. *Limnol. Oceanogr.* **67**, 1577–1589. (doi:10.1002/lno.12152)
67. Hily C, Raffin C, Brun A, den Hartog C. 2002 Spatio-temporal variability of wasting disease symptoms in eelgrass meadows of Brittany (France). *Aquat. Bot.* **72**, 37–53. (doi:10.1016/S0304-3770(01)00195-4)
68. Christiaen B, Ferrier L, Dowty P, Gaeckle J, Berry H. 2022 Puget Sound Seagrass Monitoring Report, monitoring year 2018–2020. Washington State Department of Natural Resources. See https://www.dnr.wa.gov/publications/aqr_nrsh_symp_monitoring_report_2018_2020_data.pdf.

69. Rappazzo BH, Eisenlord ME, Graham OJ, Aoki LR, Dawkins PD, Harvell D, Gomes C. 2021 EeLISA: Combating global warming through the rapid analysis of eelgrass wasting disease. *Proc. AAAI Conf. Artificial Intelligence* **35**, 15156-15165. (doi:10.1609/aaai.v35i17.17779)
70. Muehlstein LK, Porter D, Short FT. 1988 *Labyrinthula* sp., a marine slime mold producing the symptoms of wasting disease in eelgrass, *Zostera marina*. *Mar. Biol.* **99**, 465–472. (doi:10.1007/BF00392553)
71. Groner ML *et al.* 2018 Oysters and eelgrass: potential partners in a high pCO_2 ocean. *Ecology* **99**, 1802–1814. (doi:10.1002/ecy.2393)
72. JPL MUR MEaSUREs Project. 2015 GHRSST level 4 MUR global foundation Sea surface temperature analysis. PO. DAAC, a NASA data repository, CA, USA.
73. R Core Team. 2020 *R: a language and environment for statistical computing*. Vienna, Austria: R Foundation for Statistical Computing.
74. Neuwirth E. 2014 RColorBrewer: ColorBrewer palettes. *R package version* **1**, 1–2. See https://cran.r-project.org/package=RColorBrewer.
75. Wickham H. 2016 *Ggplot2: elegant graphics for data analysis*. New York, NY: Springer-Verlag.
76. Kassambara A. 2020 ggpubr: 'ggplot2' based publication ready plots. See https://cran.r-project.org/package=ggpubr.
77. Zuur AF, Ieno EN. 2016 A protocol for conducting and presenting results of regression-type analyses. *Methods Ecol. Evol.* **7**, 636–645. (doi:10.1111/2041-210X.12577)
78. Brooks M, Kristensen K, van Benthem K, Magnusson A, Berg C, Nielsen A, Skaug H, Maechler M, Bolker B. 2017 glmmTMB balances speed and flexibility among packages for zero-inflated generalized linear mixed modeling. *R J.* **9**, 378–400.
79. Bates D, Maechler M, Bolker B, Walker S. 2015 Fitting linear mixed-effects models using lme4. *J. Stat. Softw.* **67**, 1–48. (doi:10.18637/jss.v067.i01)
80. Beca-Carretero P, Stanschewski CS, Julia-Miralles M, Sanchez-Gallego A, Stengel DB. 2019 Temporal and depth-associated changes in the structure, morphometry and production of near-pristine *Zostera marina* meadows in western Ireland. *Aquat. Bot.* **155**, 5–17. (doi:10.1016/j.aquabot.2019.02.003)
81. Barton K. 2022 MuMIn: multi-model inference. See https://cran.r-project.org/package=MuMIn.
82. Hartig F. 2021 DHARMa: residual diagnostics for hierarchical (multi-level/mixed) regression models. See https://cran.r-project.org/package=DHARMa.
83. Warton DI, Hui FKC. 2011 The arcsine is asinine: the analysis of proportions in ecology. *Ecology* **92**, 3–10. (doi:10.1890/10-0340.1)
84. Ludecke D. 2021 sjPlot: data visualization for statistics in social science. See https://cran.r-project.org/package=sjPlot.
85. Menning DM, Gravley HA, Cady MN, Pepin D, Wyllie-Echeverria S, Ward DH, Talbot SL. 2021 Metabarcoding of environmental samples suggest wide distribution of eelgrass (*Zostera marina*) pathogens in the north Pacific. *Metabarcoding Metagenomics* **5**, e62823. (doi:10.3897/mbmg.5.62823)
86. Newton J, Mickett J, Manalang D, Carini R. 2022 Salish Sea ORCA buoy observations over the last decade: warmer and saltier than normal anomalies and their persistence. *Poster presented at the* Salish Sea Ecosystem Conference, *26-28 April 2022, virtual.* Washington, WA: Western Washington University's Salish Sea Institute.
87. Zimmerman RC. 2007 Light and photosynthesis and seagrass meadows. In *Seagrasses biology, ecology, and conservation* (eds AWD Larkum, RJ Orth, RM Duarte), pp. 303–321. Dordrecht, The Netherlands: Springer.
88. Giesen WBJT, Van Katwijk MM, Den Hartog C. 1990 Temperature, salinity, insolation and wasting disease of eelgrass (*Zostera marina* L.) in the Dutch Wadden Sea in the 1930's. *Neth. J. Sea Res.* **25**, 395–404. (doi:10.1016/0077-7579(90)90047-K)
89. Jakobsson-Thor S, Brakel J, Toth GB, Pavia H. 2020 Complex interactions of temperature, light and tissue damage on seagrass wasting disease in *Zostera marina*. *Front. Mar. Sci.* **7**, 575183. (doi:10.3389/fmars.2020.575183)
90. Lee K-S, Park SR, Kim YK. 2007 Effects of irradiance, temperature, and nutrients on growth dynamics of seagrasses: a review. *J. Exp. Mar. Biol. Ecol.* **350**, 144–175. (doi:10.1016/j.jembe.2007.06.016)
91. McKone K, Tanner C. 2009 Role of salinity in the susceptibility of eelgrass *Zostera marina* to the wasting disease pathogen *Labyrinthula zosterae*. *Mar. Ecol. Prog. Ser.* **377**, 123–130. (doi:10.3354/meps07860)
92. Martin DL, Boone E, Caldwell MM, Major KM, Boettcher AA. 2009 Liquid culture and growth quantification of the seagrass pathogen, *Labyrinthula* spp. *Mycologia* **101**, 632–635. (doi:10.3852/08-171)
93. MacCready P, McCabe RM, Siedlecki SA, Lorenz M, Giddings SN, Bos J, Albertson S, Banas NS, Garnier S. 2021 Estuarine circulation, mixing, and residence times in the Salish sea. *J. Geophys. Res. Oceans* **126**, e2020JC016738. (doi:10.1029/2020JC016738)
94. Lapointe BE, Herren LW, Brewton RA, Alderman PK. 2020 Nutrient over-enrichment and light limitation of seagrass communities in the Indian River Lagoon, an urbanized subtropical estuary. *Sci. Total Environ.* **699**, 134068. (doi:10.1016/j.scitotenv.2019.134068)
95. Godet L, Fournier J, van Katwijk M, Olivier F, Le Mao P, Retière C. 2008 Before and after wasting disease in common eelgrass *Zostera marina* along the French Atlantic coasts: a general overview and first accurate mapping. *Dis. Aquat. Organ.* **79**, 249–255. (doi:10.3354/dao01897)
96. Lucas GB, Campbell CL, Lucas LT. 1992 Causes of plant diseases. In *Introduction to plant diseases: identification and management* (eds GB Lucas, CL Campbell, LT Lucas), pp. 9–14. Boston, MA: Springer US.
97. Aoki LR, McGlathery KJ, Wiberg PL, Al-Haj A. 2020 Depth affects seagrass restoration success and resilience to marine heat wave disturbance. *Estuaries Coasts* **43**, 316–328. (doi:10.1007/s12237-019-00685-0)
98. Larkum AWD, Orth RJ, Duarte CM (eds) 2006 *Seagrasses: biology, ecology, and conservation*. Dordrecht, The Netherlands: Springer.
99. Lefcheck JS, Wilcox DJ, Murphy RR, Marion SR, Orth RJ. 2017 Multiple stressors threaten the imperiled coastal foundation species eelgrass (*Zostera marina*) in Chesapeake Bay, USA. *Glob. Change Biol.* **23**, 3474–3483. (doi:10.1111/gcb.13623)
100. Anderson PK, Cunningham AA, Patel NG, Morales FJ, Epstein PR, Daszak P. 2004 Emerging infectious diseases of plants: pathogen pollution, climate change and agrotechnology drivers. *Trends Ecol. Evol.* **19**, 535–544. (doi:10.1016/j.tree.2004.07.021)
101. Altizer S, Ostfeld RS, Johnson PTJ, Kutz S, Harvell CD. 2013 Climate change and infectious diseases: from evidence to a predictive framework. *Science* **341**, 514–519. (doi:10.1126/science.1239401)
102. Groner ML *et al.* 2016 Managing marine disease emergencies in an era of rapid change. *Phil. Trans. R. Soc. B* **371**, 20150364. (doi:10.1098/rstb.2015.0364)
103. Meehl GA. 2004 More intense, more frequent, and longer lasting heat waves in the 21st century. *Science* **305**, 994–997. (doi:10.1126/science.1098704)
104. Graham OJ *et al.* 2023 Data and code from: Deeper habits and cooler temperatures moderate a climate-driven disease in an essential marine habitat. Cornell University eCommons Repository. (https://doi.org/10.7298/6ybh-w566)
105. Graham OJ *et al.* 2023 Deeper habitats and cooler temperatures moderate a climate-driven seagrass disease. Figshare. (doi:10.6084/m9.figshare.c.6360115)